



HAL
open science

Photosynthetic Light Reactions in Diatoms. I. The Lipids and Light-Harvesting Complexes of the Thylakoid Membrane

Claudia Büchel, Reimund Goss, Benjamin Bailleul, Douglas Campbell,
Johann Lavaud, Bernard Lepetit

► To cite this version:

Claudia Büchel, Reimund Goss, Benjamin Bailleul, Douglas Campbell, Johann Lavaud, et al.. Photosynthetic Light Reactions in Diatoms. I. The Lipids and Light-Harvesting Complexes of the Thylakoid Membrane. *The Molecular Life of Diatoms*, Springer International Publishing, pp.397-422, 2022, 10.1007/978-3-030-92499-7_15 . hal-03672196

HAL Id: hal-03672196

<https://hal.science/hal-03672196>

Submitted on 19 May 2022

HAL is a multi-disciplinary open access archive for the deposit and dissemination of scientific research documents, whether they are published or not. The documents may come from teaching and research institutions in France or abroad, or from public or private research centers.

L'archive ouverte pluridisciplinaire **HAL**, est destinée au dépôt et à la diffusion de documents scientifiques de niveau recherche, publiés ou non, émanant des établissements d'enseignement et de recherche français ou étrangers, des laboratoires publics ou privés.

1 Chapter 1: Photosynthetic light reactions in diatoms. I. The
2 lipids and light-harvesting complexes of the thylakoid
3 membrane

4 Claudia Büchel^{1*}, Reimund Goss^{2*}, Benjamin Bailleul³, Douglas A. Campbell⁴,
5 Johann Lavaud^{5,6}, Bernard Lepetit⁷

6 * equal contribution

7 1 Institute of Molecular Biosciences, Goethe University Frankfurt, 60438 Frankfurt, Germany

8 2 Institute of Biology, Leipzig University, 04103 Leipzig, Germany

9 3 Laboratoire de Biologie du Chloroplaste et Perception de la Lumière chez les Micro-algues,
10 UMR7141, IBPC, CNRS- Sorbonne Université, Paris, France

11 4 Department of Biology, Mount Allison University, NB, Canada

12 5 UMI3376 Takuvik, CNRS/ULaval, Département de Biologie, Université Laval, Pavillon Alexandre-
13 Vachon, 1045 avenue de la Médecine, Québec (Qc) G1V0A6, Canada

14 6 Present address: UMR6539 LEMAR, CNRS/Univ Brest/Ifremer/IRD, Institut Européen de la Mer,
15 Technopôle Brest-Iroise, rue Dumont d'Urville, 29280 Plouzané, France

16 7 Plant Ecophysiology, Department of Biology, University of Konstanz, 78457 Konstanz, Germany

17 Correspondences: c.buechel@bio.uni-frankfurt.de; rgoss@rz.uni-leipzig.de

18

19

20 **Abstract**

21 Light harvesting and photochemistry is performed by photosystems coupled to specific
22 antennae embedded in the thylakoid membrane, a common principle across diatoms, plants and
23 green algae. Still, unique features of diatoms within this common principle have been unraveled
24 in recent decades, likely resulting from the complex evolutionary history of diatoms. These
25 unique features are found in (i) the lipid composition of the thylakoid membrane, ii) the spatial
26 organization of the light harvesting complexes, and iii) their protein and pigment composition.
27 This chapter summarizes current knowledge of these three specific features, with a focus on
28 structural and functional properties.

29

30

31

32

33 *Key words: diatoms, FCP, LHC, light harvesting, lipids, thylakoids, xanthophyll cycle*

34	Table of content
35	<i>p4: Introduction</i>
36	<i>p6: 1. Thylakoid lipids</i>
37	<i>p6: 1.1 The lipid composition of thylakoid membranes</i>
38	<i>p8: 1.2 Fatty acid composition of thylakoid membrane lipids</i>
39	<i>p9: 1.3 Function of thylakoid membrane lipids</i>
40	<i>p11: 1.4 Localization of thylakoid membrane lipids</i>
41	<i>p13: 2. Light harvesting</i>
42	<i>p13: 2.1 The diatom light harvesting systems</i>
43	<i>p14: 2.2 Subunit compositions of light harvesting complexes</i>
44	<i>p15: 2.3 FCPs associated with PSI</i>
45	<i>p16: 2.4 FCPs associated with PSII</i>
46	<i>p18: 2.5 Molecular structure of FCPs</i>
47	<i>p20: 2.6 Excitation energy transfer in FCPs</i>
48	<i>p23: Outlook</i>
49	<i>p24: References</i>
50	<i>p31: Acknowledgements</i>
51	

52 **Abbreviations**

- 53 *C. meneghiniana*: *Cyclotella meneghiniana*
54 *Ch. gracilis*: *Chaetoceros gracilis*
55 Chl: chlorophyll
56 Dd: diadinoxanthin
57 DGDG: digalactosyldiacylglycerol
58 DGGC: diacylglycerylcarboxyhydroxymethylcholine
59 DGTA: diacylglycerylhydroxymethyl-N,N,N-trimethyl- β -alanine
60 DGTS: diacylglyceryl-N-trimethylhomoserine
61 DHA: docosahexaenoic acid
62 Dt: diatoxanthin
63 EPA: eicosapentaenoic acid
64 FCP: fucoxanthin-chlorophyll-protein complex
65 Fx: fucoxanthin
66 H_{II}: inverted hexagonal phase
67 *H. ostrearia*: *Haslea ostrearia*
68 ICT: intramolecular charge transfer
69 LHC: light-harvesting complex
70 MGDG: monogalactosyldiacylglycerol
71 *P. tricorutum*: *Phaeodactylum tricorutum*
72 PG: phosphatidylglycerol
73 PSI: photosystem I
74 PSII: photosystem II
75 PUFAs: polyunsaturated fatty acids
76 qE: energy dependent quenching
77 SQDG: sulphoquinovosyldiacylglycerol
78 *T. pseudonana*: *Thalassiosira pseudonana*
79 XC: xanthophyll cycle
80

81

82 **Introduction**

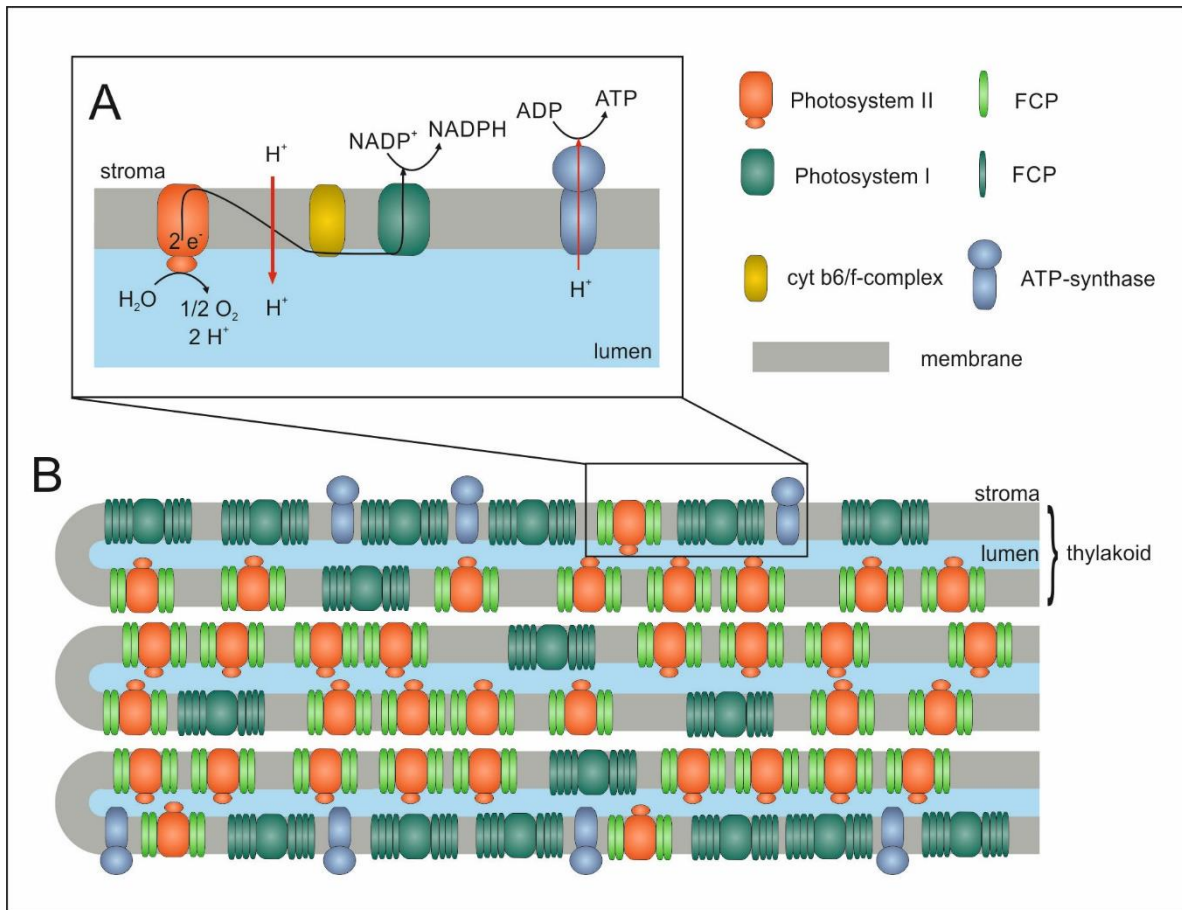
83 Diatoms perform oxygenic photosynthesis, whereby the basic reactions are identical in all
84 eukaryotes: light energy is absorbed by the pigments bound to photosystem (PS) I and II and
85 their associated light-harvesting complexes (LHC). It is transferred to special chlorophyll (Chl)
86 *a* molecules in the PS, the so-called reaction center Chls, where charge separation takes place.
87 This fuels the photosynthetic electron transport, where electrons are subtracted from water and
88 eventually used for the generation of NADPH (Fig. 1A). These photosynthetic light reactions
89 take place in the thylakoid membranes, and the coupling of the electron transfer to a
90 unidirectional transport of protons leads to accumulation of protons in the lumen that is used
91 by an ATP-Synthase to generate ATP (for details see “*Photosynthetic light reactions in diatoms.*
92 *II. The dynamic regulation of the various light reactions*”). NADPH and ATP are then mainly
93 used by the Calvin cycle in the chloroplast stroma to fix CO₂. Thus, diatoms share the same
94 elementary photosynthetic modules with other organisms performing oxygenic photosynthesis
95 (Falkowski et al. 2008), which are fairly similar in all eukaryotes, with one exception: Light-
96 harvesting systems differ significantly amongst the different taxa (Neilson and Durnford 2010,
97 Büchel 2015, Büchel 2020, Croce and van Amerongen, 2020). In addition, there are further
98 subtle changes concerning photosystems and their functional organization. For example, the
99 PSII core recently crystallized from *Chaetoceros gracilis* contains four more Chl *a* molecules
100 than the plant PSII core, and one additional subunit shielding the oxygen evolving complex
101 (Nagao et al. 2019a). With more than 100,000 species of diatoms present on earth, exhibiting a
102 huge phylogenetic diversity (Mann and Vanormelingen 2013), we may also assume some
103 diversity among diatom species even within these elementary modules.

104 The photosynthetic modules are embedded in the thylakoid membrane. In contrast to the green
105 lineage, diatom thylakoids are organized in homogeneous stacks of three which run along the
106 whole diatom plastid (Berkaloff et al. 1990) (Fig. 1B). They do not show the grana stroma
107 differentiation which imposes the lateral segregation of the PSII and PSI in plants (Anderson
108 1999). In diatoms, immunolocalization studies, lipid analyses, and 3D reconstruction showed
109 that PSI are mostly found in the stroma-facing external thylakoids whereas PSII are embedded
110 in the core of the stack, at the interface of two thylakoids (Pyszniak and Gibbs 1992; Lepetit et
111 al. 2012; Flori et al. 2017). This heterogeneity is enforced under red light conditions, which
112 induce an unusual stacking of diatom thylakoids. Here, large areas were revealed which are
113 exclusively occupied by PSI supercomplexes consisting of PSI cores with their PSI-specific
114 antenna of Lhc proteins (Bína et al. 2016). In line with this, clusters of PSII cores including
115 their FCP antennae have been revealed by cryo-electron tomography in *Phaeodactylum*

116 *tricornutum* recently (Levitani et al. 2019). For steric reasons the ATP synthase is located in the
117 outer thylakoids. The vicinity of PSII and PSI, as well as some connections between thylakoids,
118 ensures a fast diffusion of electron shuttles between the two photosystems (Flori et al. 2017),
119 whereas their diffusion can limit the overall rate of the linear electron flow in plants (Kirchhoff
120 et al. 2004; Kirchhoff et al. 2011). This peculiar segregation also has important consequences
121 for the regulation of the light capture by the two photosystems, by preventing the share of
122 excitons between them (Flori et al. 2017), a process found in cyanobacteria and red algae, and
123 called spillover (Biggins and Bruce 1989). Whether based on immunoblot quantification or
124 functional measurements, diatoms seem to possess more PSII than PSI, in contrast to plants and
125 green algae where PSI occurs at least in the same amount as PSII (Smith and Melis 1988;
126 Strzepak and Harrison 2004; Thamatrakoln et al. 2013). With this higher amount of PSII,
127 diatoms may compensate their slightly lower maximum PSII efficiency, which is usually
128 around 0.6-0.7, while in plants it reaches values of ~0.84 (Kalaji et al. 2014).

129 Lipids and pigmented proteins are the major components of the diatom thylakoid membrane.
130 Usually, the proteins occupy an area of 70-80 % of the thylakoid membrane, while lipids
131 correspondingly contribute to 20-30 % (Kirchhoff 2014). Compared to the green lineage, both
132 the respective amounts of the different thylakoid lipid classes and the respective fatty acids
133 composition is considerably different in diatoms. Moreover, the structure and composition of
134 the light harvesting system, the dominant protein constituent of the thylakoid membranes,
135 shows various diatom specific peculiarities. Certainly one reason for these differences is based
136 on the complex evolutionary history of diatoms - with plastids originating from secondary
137 endosymbiosis with red algae, while considerable amounts of 'green' genes are also found in
138 the diatom genome (Dorrell et al. 2017).

139 In this review article, we will summarize current knowledge on lipid composition (part 1) and
140 antennae structures of diatom thylakoids (part 2).



141

142 **Figure 1:** (A) General, simplified scheme of the light reactions of photosynthesis. Only PSII
 143 (red) cytb6/f complex (yellow), PSI (green) and ATPsynthase (blue) are shown. Light-
 144 harvesting systems have been omitted since they differ significantly between the different algal
 145 groups and higher plants. For more detail on electron and proton transfer refer to Figure 1 in
 146 chapter “*Photosynthetic light reactions in diatoms. II. The dynamic regulation of the various*
 147 *light reactions*”. (B) Scheme of the thylakoid membrane structure of diatoms (B). The
 148 thylakoids are organized in stacks of three that span the whole plastid. The outer membranes of
 149 such stack are enriched in PSI, whereas PSII is predominantly found in the inner four
 150 membranes. Cytb6/f complexes that are not preferentially localized (Flori et al. 2017) have been
 151 omitted as well as connections between thylakoids of one stack. In diatoms the light-harvesting
 152 complexes are called fucoxanthin-chlorophyll proteins (FCP). FCPs tightly bound to PSII are
 153 shown in light green, FCPs belonging to PSI are shown in dark green.

154

155

156 1. Thylakoid lipids

157 1.1 The lipid composition of thylakoid membranes

158 Before the lipid and fatty acid composition of diatom thylakoid membranes is presented in
 159 detail, it should be mentioned that most of the depicted results have been derived from
 160 laboratory experiments under defined growth conditions (for details please refer to the cited
 161 references). However, in their natural environment diatoms are exposed to extreme differences

162 in temperature and light intensities. To cope with these extreme abiotic conditions diatoms
163 adjust the lipid and fatty acid composition of the thylakoids in order to maintain the membrane
164 in a fluid working state (see also 1.2 and 1.3).

165 The diatom thylakoid membranes are composed of the two neutral galactolipids
166 monogalactosyldiacylglycerol (MGDG) and digalactosyldiacylglycerol (DGDG), the
167 negatively charged sulfolipid sulphoquinovosyldiacylglycerol (SQDG) and the anionic
168 phospholipid phosphatidylglycerol (PG) (Vieler et al. 2007; Goss et al. 2009; Lepetit et al.
169 2012; Abida et al. 2015). These lipids are also found in higher plants, but in addition the diatom
170 thylakoid membranes can contain low amounts of betaine lipids like
171 diacylglycerylcarboxyhydroxymethylcholine (DGGC) and diacylglycerylhydroxymethyl-
172 N,N,N-trimethyl- β -alanine (DGTA) (Vieler et al. 2007; Canavate et al. 2016). A third betaine
173 lipid, namely diacylglyceryl-N-trimethylhomoserine (DGTS), which acts as precursor in the
174 synthesis of DGTA, can be found in trace amounts (Canavate et al. 2016). Phosphatidylcholine,
175 which in higher plant thylakoid preparations is supposed to represent a contamination with
176 chloroplast envelope membranes, seems to be a general constituent of diatom thylakoid
177 membranes (Vieler et al. 2007; Goss et al. 2009; Lepetit et al. 2012).

178 Although the main lipids of diatom thylakoids are comparable to those of the green lineage,
179 their contribution to the overall lipid content of the membrane is significantly different. While
180 in higher plants and green algae the neutral galactolipids dominate the lipid content of the
181 thylakoid membrane and amount to 70 to 80% of the total lipid (Murata and Siegenthaler 1998),
182 the concentrations of MGDG and DGDG are strongly reduced in the thylakoids of pennate (*P.*
183 *tricornutum*) and centric (*Cyclotella meneghiniana*) diatoms (Goss et al. 2009; Lepetit et al.
184 2012; Abida et al. 2015). The reduction of MGDG and DGDG is accompanied by simultaneous
185 increases of the two negatively charged lipids SQDG and PG. This is especially obvious in
186 thylakoid membranes of *P. tricornutum* or *C. meneghiniana* purified from high light grown
187 cultures (Lepetit et al. 2012). They contain SQDG as the most abundant lipid, and the combined
188 negatively charged lipids SQDG and PG contribute to more than 50% of the total thylakoid
189 lipids. The ratio of neutral to negatively charged lipids lies between one and two and is thus
190 significantly lower than the typical values between three and four observed in higher plant and
191 green algal thylakoid membranes. High concentrations of the negatively charged lipids SQDG
192 and PG in diatom thylakoid membranes are supported by the study of Yan et al. (2011) who
193 determined the photosynthetic lipid and fatty acid profile of three different strains of the marine
194 diatom *Skeletonema* sp.. Two of the three strains show high SQDG concentrations (35-40% of

195 the photosynthetic lipids) and, in combination with PG, the negatively charged lipids amount
196 to almost 50% of the total photosynthetic lipids of *Skeletonema*.

197 ***1.2 Fatty acid composition of thylakoid membrane lipids***

198 Diatoms are characterized by the synthesis of very long-chain polyunsaturated fatty acids
199 (PUFAs) with chain lengths of up to 28 C atoms (Guschina and Harwood 2006). The presence
200 of long-chain PUFAs is also reflected by the fatty acid composition of the thylakoid membrane
201 lipids. In centric diatoms (*Skeletonema marinoi*, *Thalassiosira weissflogii*) and the pennate *P.*
202 *tricornutum* MGDG contains the main long-chain PUFA of diatoms, i.e. eicosapentaenoic acid
203 (EPA, 20:5) (Yongmanitchai and Ward 1993; Yan et al. 2011; Dodson et al. 2013; Dodson et
204 al. 2014; Abida et al. 2015). EPA is preferentially bound to the sn-1 position of the glycerol
205 backbone whereas C16 fatty acids with different amounts of double bonds (16:1, 16:2, 16:3,
206 16:4) can be observed at the sn-2 position. MGDG with C20:5 and C16:3 fatty acids seems to
207 represent the majority of MGDG molecules in diatom thylakoids. Interestingly, EPA at the sn-
208 1 position of the MGDG molecule can be replaced by other C20 fatty acids with a lower amount
209 of double bonds like eicosatrienoic acid (20:3) or eicosatetraenoic acid (20:4). In addition to
210 MGDG molecules with C20/C16 fatty acids, the recent analyses have presented evidence for
211 the presence of MGDG molecules with C16 fatty acids at both the sn-1 and sn-2 position.
212 Longer-chain PUFAs, like docosahexaenoic acid (DHA, 22:6), or C18 fatty acids are usually
213 not found or detected in only minor concentrations in MGDG of centric diatoms and *P.*
214 *tricornutum*.

215 The analyses by Yongmanitchai and Ward (1993), Yan et al. (2011), Dodson et al. (2013),
216 Dodson et al. (2014) & Abida et al. (2015) also pointed out that the fatty acid composition of
217 the main galactolipids MGDG and DGDG is comparable. EPA is the main fatty acid species at
218 the sn-1 position of the DGDG molecule. The sn-2 position of DGDG is usually occupied by
219 C16 fatty acids, and DGDG forms with C16 fatty acids at both the sn-1 and sn-2 positions can
220 be observed. Like MGDG, DGDG molecules with the two fatty acids EPA (C20:5) and
221 hexadecatrienoic acid (C16:3) seem to represent the majority of DGDG molecules in the diatom
222 thylakoid membrane. Other pennate diatoms (*Haslea ostrearia* and *Navicula perminuta*) seem
223 to exhibit a different fatty acid composition of the MGDG and DGDG molecules compared
224 with the centric diatoms and *P. tricornutum* (Dodson et al. 2013). In these species, an
225 enrichment of EPA cannot be detected and C18/C16 and C18/C18 forms of MGDG and DGDG
226 are typically observed. The major forms of MGDG and DGDG seem to contain linolenic acid
227 (18:3) and hexadecatrienoic acid (16:3) at the sn-1 and sn-2 positions, respectively. The fatty

228 acid composition of these pennate diatoms thus is comparable to the fatty acid composition of
229 MGDG and DGDG of higher plants and green algae (Browse et al. 1986; Cho and Thompson
230 1987). However, this different lipid profile may be related to acclimation to environmental
231 temperatures. Indeed, Dodson et al. (2014) could detect significant amounts of EPA in *H.*
232 *ostrearia* at the sn-1 position of the MGDG and DGDG molecules under normal temperature
233 conditions, whereas at high temperatures (30 °C) no EPA or other C20 fatty acids, but high
234 concentrations of C18 fatty acids could be observed at the sn-1 position of MGDG and DGDG
235 both in *H. ostrearia* and also *P. tricornutum*.

236 With regard to the anionic membrane lipids of diatoms, the fatty acid composition of SQDG of
237 *P. tricornutum* (Yongmanitchai and Ward 1993; Abida et al. 2015) and that of SQDG and PG
238 of three *Skeletonema* species has been analyzed (Yan et al. 2011). In contrast to MGDG and
239 DGDG, the main part of SQDG present in diatom thylakoid membranes is enriched in fatty
240 acids with a shorter chain length and C14 and C16 fatty acids are usually observed in both the
241 sn-1 and sn-2 positions. The C14 and C16 fatty acids include C14:0, C16:0, C16:1 and C16:3
242 species. PG in *Skeletonema*, on the other hand, contains C18:1 fatty acids as the main molecular
243 species.

244 ***1.3 Function of thylakoid membrane lipids***

245 Thylakoid membrane lipids exert their functions on different structural levels. First, they build
246 up the membrane bilayer in which the photosynthetic pigment protein complexes and the
247 components of the electron transport chain are incorporated. Changes in the lipid and/or fatty
248 acid composition of the thylakoid membrane as a reaction to changes in the environmental
249 conditions, like e.g. temperature or light fluctuations, keep the membrane in a fluid state and
250 thus maintain efficient electron transport and other membrane related processes such as the
251 operation of the diadinoxanthin cycle (see below). The importance of a fluid state for the
252 operation of biological membranes has first been described by Singer and Nicolson (1972).
253 Recently, advances in our understanding of the fluid mosaic model with a special focus of
254 different lipid phases in thylakoid membranes have been presented by Wilhelm et al. (2020).

255 With respect to the environmental factor light, Mock and Kroon (2002) observed an increase
256 of the non-bilayer lipid MGDG accompanied by higher concentrations of EPA in sea ice
257 diatoms which were grown under low light illumination. They proposed that the high contents
258 of EPA were responsible for membrane fluidity and the velocity of the photosynthetic electron
259 transport. Rousch et al. (2003) observed that the thermo-tolerant diatom *Chaetoceros muelleri*
260 reacted with stronger changes in the fatty acid profile to temperature changes than the thermo-

261 intolerant *P. tricornutum*. Recently, Bojko et al. (2017) could show that the centric diatom
262 *Thalassiosira pseudonana* reacted with an increase of PUFAs to a decrease of the cultivation
263 temperature. The higher content of PUFAs resulted in a stabilization of the membrane fluidity
264 and the PSII quantum yield at low temperatures. In addition to their role as membrane building
265 blocks, thylakoid lipids serve as structural elements of the pigment proteins and play a role in
266 the oligomerization of photosystems and light-harvesting complexes. Through an enrichment
267 at the monomer-monomer interface MGDG seems to play a role in the establishment and
268 maintenance of PSII dimers which represent the native state of PSII in the thylakoid membrane
269 (Kern and Guskov 2011; Nagao et al. 2019a). PG is most likely involved in the trimerization of
270 the PSII light-harvesting complex of higher plants, the LHCII, whereas DGDG is important for
271 the structural integrity of the complex (Kühlbrandt et al. 1994).

272 Recently, the first molecular structure of a diatom pigment protein complex determined by x-
273 ray crystallography has been published, namely that of the dimeric fucoxanthin chlorophyll
274 binding protein (FCP) complex of *P. tricornutum* (Wang et al. 2019) (see “2.5 Molecular
275 structure of FCPs”). Within the dimeric FCP two lipid molecules have been resolved, a PG and
276 a DGDG molecule. Although the PG and DGDG molecules have not been assigned specific
277 roles in the dimerization of the FCP, it was proposed that the two lipid molecules serve to
278 stabilize the FCP dimers. The determination of the structure of a PSII-FCP supercomplex from
279 the pennate diatom *Ch. gracilis* by cryo-electron microscopy revealed the presence of more
280 than 100 lipid molecules in the PSII-FCP dimer (Pi et al. 2019; Wang et al. 2020). The majority
281 of the lipids, comprising 20 DGDG, 42 MGDG, 16 SQDG and 30 PG molecules, are located at
282 the interfaces of the PSII protein subunits which, according to Wang et al. (2020), argues for
283 an important role in the establishment and stabilization of protein subunit interactions. A
284 stabilizing role of thylakoid membrane lipids for the native structure of FCP complexes has also
285 been reported in another study (Schaller-Laudel et al. 2017). In these experiments, the neutral
286 galactolipids MGDG and DGDG exhibited the highest capacity for the stabilization of FCP
287 complexes. For higher plants and cyanobacteria it has been shown that MGDG plays a role in
288 targeting Q_B to its binding site at the stromal side of the PSII reaction center and that DGDG is
289 important for the stabilization of the Oxygen Evolving Complex at the luminal side of PSII
290 (Kern and Guskov 2011). Although the first results concerning the structure of the diatom PSII
291 core complex have been published (Wang et al. 2020), a detailed assignment of the lipid
292 molecules within the core complex to specific functions is still missing. However, the structural
293 and functional similarities between the diatom and higher plant and cyanobacterial PSII and
294 PSI core complexes suggest a similar role of the thylakoid lipids in photosystems of diatoms.

295 Besides the lipids that build up the main lipid phase of the thylakoid membrane and those that
296 serve as structural lipids embedded into the protein matrix, a third class of membrane lipids
297 exist. These lipids are closely associated with the pigment protein complexes and form a lipid
298 shield surrounding the complexes. In the LHCII of higher plants (Schaller et al. 2010) and the
299 FCP complexes of the diatoms *P. tricornutum* and *C. meneghiniana* (Lepetit et al. 2010) the
300 lipid shields are highly enriched in MGDG. MGDG serves to solubilize the hydrophobic
301 xanthophyll cycle (XC) pigments violaxanthin, antheraxanthin and zeaxanthin in higher plants
302 and diadinoxanthin (Dd) and diatoxanthin (Dt) in diatoms, thereby making these pigments
303 accessible to the enzymes violaxanthin or diadinoxanthin de-epoxidase (Goss et al. 2005; Goss
304 et al. 2007). (*Side note: The diadinoxanthin de-epoxidase is usually annotated as a violaxanthin*
305 *de-epoxidase in diatom genomes. This reflects the fact that this enzyme can also de-epoxidize*
306 *violaxanthin, which is a precursor in synthesis of the main diatom carotenoids fucoxanthin and*
307 *Dd (Lohr and Wilhelm 1999).)* The XC has a dominant role in photoprotection of plants and
308 diatoms (see “*Photosynthetic light reactions in diatoms. II. The dynamic regulation of the*
309 *various light reactions*”). It has also been proposed that the local enrichment of MGDG leads
310 to the establishment of a special lipid phase, the so-called inverted hexagonal (H_{II}) phase. This
311 non-bilayer phase seems to be essential for the efficient conversion of XC pigments (Latowski
312 et al. 2002; Latowski et al. 2004; Goss et al. 2005; Goss et al. 2007). The H_{II} phase together
313 with the LHCII/FCP, the de-epoxidases and the XC pigments can be described as a special
314 thylakoid membrane domain with a specific lipid and protein composition and a specific
315 function, namely the enzymatic de-epoxidation of the XC pigments (Goss et al. 2017).
316 The XC pigments also influence the properties of the lipid phase of the membrane. The
317 conversion of Dd to Dt leads to a stable increase of the rigidity of the hydrophobic core of the
318 diatom thylakoid membrane and a dynamic stabilization of the peripheral membrane parts
319 which can be observed during the ongoing de-epoxidation reaction (Bojko et al. 2019). The
320 stabilization of diatom thylakoids by XC pigments has been suggested to play a role in the
321 adaptation of the membrane to rapid changes in temperature.

322

323 ***1.4 Localization of thylakoid membrane lipids***

324 Based on the findings that SQDG strongly inhibits the de-epoxidation of Dd to Dt (Goss et al.
325 2009) and that MGDG forms a lipid shield around the FCP complexes, which incorporates a
326 large part of the XC pigments (Lepetit et al. 2010), a model for the lipid and protein distribution
327 in the thylakoid membranes of diatoms was proposed (Lepetit et al. 2012). The model predicts

328 that the inner membranes of the typical stacks of three thylakoids are enriched in PSII and its
329 associated FCP complexes (Fig. 1). The lipid composition of the inner membranes is dominated
330 by MGDG and represents the place where efficient operation of the XC is taking place. SQDG,
331 on the other hand, is enriched in the outer membranes of the thylakoid stacks so as not to
332 interfere with the diadinoxanthin de-epoxidase. Outer membranes and margin regions of the
333 stacks contain mainly PSI and the ATP synthase which thus gains access to the chloroplast
334 stroma. Although the model was mainly based on physiological and biochemical data, recent
335 structural data have confirmed several important aspects and predictions (Flori et al. 2017) (see
336 also "*Introduction*"). Revealing also connections between the different thylakoid lamellae, the
337 authors concluded that the three-dimensional network of the thylakoid membrane of diatoms is
338 far more complex than the simple layout of three loosely connected membranes.

339

340

341 **2. Light harvesting**

342 Diatoms, like vascular plants, harvest light using membrane intrinsic proteins that belong to the
343 light-harvesting complex (Lhc) protein family. Lhcs are characterized by three membrane
344 spanning α -helices, whereby helix 1 and 3 form a cross-like superhelical structure. These
345 proteins non-covalently attach chlorophylls (Chl) as well as carotenoids. Lhcs are connected
346 with the photosystem core complexes, forming so-called photosystem supercomplexes. Major
347 differences compared to plants can be found in the number of Lhcs associated with the
348 photosystems, their specific structure, and the number and identity of pigments bound to the
349 diatom light harvesting apparatus. In recent years there have been major advances in
350 understanding the light harvesting machinery of diatoms which we will review here.

351

352 ***2.1 The diatom light harvesting systems***

353 In diatoms Lhcs, Chl *a* and Chl *c*₁ (and little Chl *c*₂) (Fawley 1989; Kraay et al. 1992) are
354 accompanied by the major carotenoid fucoxanthin (Fx), and usually by minor amounts of Dd
355 and Dt. The diatom genome encodes large numbers of *Lhc* genes whose translated proteins fall
356 into three major and some minor groups. The major groups include i) the main group of proteins
357 working in light harvesting, named *Lhcf*, ii) Lhcs most closely related to those of red algae
358 called *Lhcr*, and iii) the photoprotective proteins called LI818 or *Lhcx*, related to green algal
359 *LhcSR* (Eppard and Rhiel 1998; Bailleul et al. 2010; Ghazaryan et al. 2016). The minor groups
360 comprise iv) a small group of genes called *Lhcz*, v) the so called *RedCaps* (Engelken et al.
361 2012), and vi) some other sequences that do not belong to either group. *Lhcf* and *Lhcr* genes
362 constitute the biggest groups with 8-17 and 9-14 members, respectively, when comparing the
363 three best studied diatoms *P. tricornutum* (Bowler et al. 2008), *T. pseudonana* (Armbrust et al.
364 2004), and *Cyclotella meneghiniana* (Gundermann et al. 2019). Concerning *Lhcx*, numbers are
365 smaller with 4-6 genes. However, numbers are even higher for e.g. *Fragilariopsis cylindrus*
366 (Mock et al. 2017). For *P. tricornutum* as well as for *T. pseudonana*, expression of all those
367 genes was proven either on mRNA or on protein level in cells and pigment-protein complexes
368 (Nymark et al. 2009; Lepetit et al. 2010; Grouneva et al. 2011; Schober et al. 2019; Kansy et
369 al. 2020), and for *C. meneghiniana* all *Lhcf* and some *Lhcx* proteins were found in different
370 light harvesting complexes (Gundermann et al. 2019). Most of the proteins encoded for by *Lhc*
371 genes assemble into multi-subunit complexes that are then called fucoxanthin-chlorophyll-
372 protein complexes (FCP). Note that single Lhc proteins of diatoms sometimes are also called

373 FCP mainly for historical reasons, since the Lhc nomenclature was only introduced when the
374 first whole genome sequences became available.

375

376 **2.2 Subunit compositions of light harvesting complexes**

377 As in vascular plants, the photosystems of diatoms are surrounded by light harvesting
378 complexes, whereby some are more tightly bound to either PSII or PSI, forming PSII-FCP or
379 PSI-FCP supercore complexes/supercomplexes, respectively. Besides, there is an additional
380 pool of more loosely bound FCPs, which will be considered first. Early on pools of FCPs were
381 isolated and characterized from the pennate diatom *P. tricornutum* (Alberte et al. 1981;
382 Friedman and Alberte 1984; Gugliemelli 1984; Fawley and Grossman 1986; Owens and World
383 1986; Caron and Brown 1987; Owens 1988; Berkaloff et al. 1990; Lavaud et al. 2003;
384 Guglielmi et al. 2005). Later, centric diatoms like *C. meneghiniana* or *T. pseudonana* were
385 studied as well, and sub-populations of FCP complexes were differentiated. In the pennate *P.*
386 *tricornutum*, only trimeric FCP complexes were found (Joshi-Deo et al. 2010; Grouneva et al.
387 2011) that, nonetheless, could interact to form yet larger complexes (Lepetit et al. 2007; Gardian
388 et al. 2014). Further separation demonstrated the presence of three major trimers, with Lhcf5,
389 Lhcf10 and Lhcf2, or Lhcf4 as main subunits, respectively, together with different other Lhcf
390 polypeptides (Gundermann et al. 2013). Later, homodimers of Lhcf4 were found in crystals
391 used for X-ray crystallography (Wang et al. 2019, see below). No members of the other Lhc
392 families (Lhcr or Lhcx) were found in purified trimeric FCPs of pennates so far (Gundermann
393 et al. 2013), although the photoprotective Lhcx as well as Lhcr proteins are present when
394 isolating the whole pool of FCP complexes (Lepetit et al. 2010; Nagao et al. 2013a; Taddei et
395 al. 2018). In contrast, trimeric and specific higher oligomeric complexes were isolated from *C.*
396 *meneghiniana*, a centric diatom (Büchel 2003), and two different complexes were later verified
397 for other centrics as well, *T. pseudonana* (Grouneva et al. 2011) and *Ch. gracilis* (Nagao et al.
398 2012; Nagao et al. 2013a), respectively. In the centrics *C. meneghiniana* and *T. pseudonana*,
399 Lhcf proteins accompanied by Lhcx1 proteins defined the major trimeric complex, named
400 FCPa. The oligomeric complex with distinct Lhcf composition, named FCPb, was proven to be
401 a nonamer (Röding et al. 2018). In *Ch. gracilis*, the oligomeric complex was named FCP-A and
402 the trimeric complex FCP-B/C due to their subunit composition (Nagao et al. 2012; Nagao et
403 al. 2013a). Recently, FCPa and FCPb complexes of *C. meneghiniana* were further divided into
404 sub-complexes (Gundermann et al. 2019). Four different trimeric FCPa complexes were shown
405 to exist, whereby FCPa3 and FCPa4 were the most abundant forms. Lhcf1 was the major
406 polypeptide in both, accompanied by Lhcx1 in case of FCPa4. For FCPb two sub-complexes

407 were distinguished: FCPb1 that is built almost solely of Lhcf3, and FCPb2 that in addition
408 contains Lhcx1 and Lhcx6_1 when isolated from cells grown under high light. When using
409 sucrose gradient centrifugation to separate solubilized thylakoid membrane proteins, two bands
410 were obtained, whereby the upper band contained associations of FCPa4, FCPa1 and FCPb2,
411 i.e. those complexes that contain Lhcx1, whereas the lower band was an association of the
412 remaining FCPa trimers and FCPb nonamers devoid of Lhcx1.

413 Lhcx1 is very similar in sequence in centrics and pennates, but only in centrics it was found in
414 FCP trimers so far. It was proven to be involved in photoprotection in whole cells in both groups
415 (Bailleul et al. 2010; Zhu and Green 2010; Ghazaryan et al. 2016; Buck et al. 2019) (see
416 *Photosynthetic light reactions in diatoms. II. The dynamic regulation of the various light*
417 *reactions*). For *C. meneghiniana* it could also be shown that suppression of the fluorescence
418 quenching of FCPa depends on Lhcx1 content, pH and aggregation (Gundermann and Büchel
419 2012), whereby Lhcx1 *in vivo* does not seem to act as direct quencher, but probably promotes
420 FCPa aggregation (Ghazaryan et al. 2016), in line with the proposed uncoupling of the
421 peripheral antennae upon induction of qE in pennates (Buck et al. 2019). Regarding the other
422 Lhcx proteins, very little is known about their specific localization in the thylakoid membrane.
423 For Lhcx3 of *P. tricornutum*, some evidence exists for a binding to the FCP complexes and to
424 PSI, but further experiments are needed to corroborate this result (Taddei et al. 2018).

425 Only pennate diatoms like *P. tricornutum* have a ‘red antenna’ when cultivated under red light
426 (Herbstová et al. 2015; Herbstová et al. 2017), characterized by a long wavelength fluorescence
427 at around 710 nm at room temperature that is attributed to PSII. The main component of this
428 red fluorescing antenna is Lhcf15, a protein which is not closely related to the other main Lhcf
429 proteins that constitute the trimers and which has no close homologue in centrics. This red-
430 shifted antenna was interpreted as an evolutionary adaptation towards survival in shaded
431 environments. Recently, however, results demonstrated that the ‘red antenna’ may also be
432 induced under weak green and yellow light (Oka et al. 2020).

433

434 **2.3 FCPs associated with PSI**

435 PSI-FCP supercores were isolated before sequences of Lhcs became known, and accordingly
436 no detailed attribution of protein isoforms to complexes was initially possible (Berkaloff et al.
437 1990; Brakemann et al. 2006; Veith and Büchel 2007; Ikeda et al. 2008). Later, the homology
438 of Lhcr with the red algal PSI antenna proteins gave rise to the assumption that Lhcr
439 polypeptides fulfill the same function. Indeed, Lhcr proteins can be found in PSI isolates (Veith
440 et al. 2009; Lepetit et al. 2010; Grouneva et al. 2011). Depending on the isolation procedure,

441 Lhcr are the sole PSI antennae components (Lepetit et al. 2010), or Lhcf (and sometimes Lhcx)
442 proteins were present in the PSI antenna as well (Brakemann et al. 2006; Veith and Büchel
443 2007; Ikeda et al. 2008; Veith et al. 2009; Grouneva et al. 2011; Juhas and Büchel 2012; Ikeda
444 et al. 2013; Calvaruso et al. 2020; Nagao et al. 2020). As in vascular plants, PSI of diatoms is
445 a monomer (Veith and Büchel 2007; Ikeda et al. 2008; Nagao et al. 2020). In *Ch. gracilis*, the
446 antenna complexes that serve PSI are characterized by long wavelength absorbing Chls that
447 rapidly equilibrate with Chls in the PSI core through uphill energy excitation transfer (Nagao
448 et al. 2018; Nagao et al. 2019b).

449 From the same organism the structure of a PSI-FCP supercomplex at 2.4 Å resolution became
450 available recently (Nagao et al. 2020). Sixteen monomeric Lhcs surround the highly conserved
451 core, i.e. much more Lhc subunits than in any other organism studied so far. Ten of those are
452 Lhcr proteins and the others belong to a group that was named Lhcq and is closely related to
453 Lhcf. The Lhc subunits are called Fcpa in the corresponding publication (Nagao et al. 2020),
454 but the respective Lhcr/Lhcq names can be found in the protein data bank file (pdb file 6L4U).
455 Nine Fcpa are surrounding the core in a circle that is almost closed (Fcpa1-9), whereby only
456 the PsaL/I side is not binding any Lhc. These Lhc all belong to the Lhcr family. On the PsaA
457 side, Fcpa10-16 are found in addition, whereby only Fcpa10 belongs to the Lhcr group, and the
458 others are Lhcq proteins. Pigment binding differs strongly between the Fcpa subunits: five to
459 thirteen Chl *a*, none to seven Chl *c*, one to seven Fx and one to four Dd are found. For example,
460 the subunit called Fcpa15 has the highest pigment load with 13 Chl *a*:0 Chl *c*:7 Fx:2 Dd,
461 whereas Fcpa1 carries only a small amount of pigments (6 Chl *a*:2 Chl *c*:2 Fx:1 Dd). Fcpa13 is
462 very unusual with a high Chl *c* and low Fx content (6:6:2:1). More recently, the structure of an
463 even bigger PSI-FCP complex from *Ch. gracilis* was solved (Xu et al. 2020). Here, 24
464 monomeric FCP surround the monomeric PSI cores. Unfortunately, neither protein nor pigment
465 attribution are identical for the FCP complexes present in both structures.

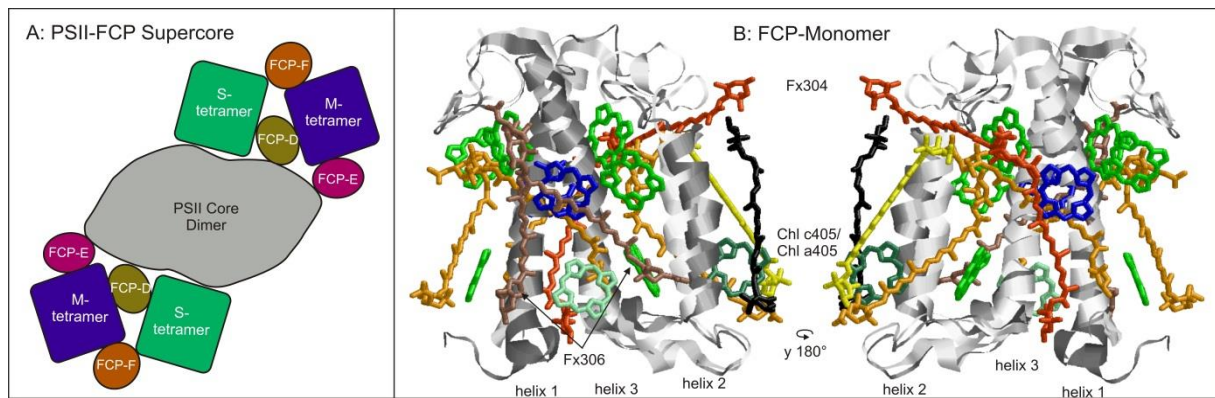
466

467 ***2.4 FCPs associated with PSII***

468 A lot of detail is also known about PSII-FCP supercores, since the structure of such a complex
469 at high resolution from *Ch. gracilis* became also available recently (Nagao et al. 2019a; Pi et
470 al. 2019). The core dimer of PSII is highly homologous to that of vascular plants and especially
471 red algae, but the organization of the surrounding FCPs differs. Diatoms lack homologues to
472 the minor antenna proteins CP24, CP26, and CP29 of plants, but nonetheless monomeric Lhc
473 are found, albeit in totally different positions. Comparable to the situation in vascular plants,
474 where light-harvesting complex II (LHCII) is found in the supercores, two strongly bound (S)

475 and two less tightly bound (M) oligomers of FCPs are present in the dimeric PSII supercores
476 (Fig. 2A). However, these FCPs are tetrameric in *Ch. gracilis*, in contrast to the trimers or
477 nonamers reported for the free pool of FCPs in the same species. Since *Ch. gracilis* is not
478 sequenced, only some Lhc sequences could be used for model building. According to Pi et al.
479 (2019), the tetramers consist of FCP-A, i.e. the polypeptide found in the nonamers of the free
480 FCP pool before. Due to the lack of sequences, the homologous sequence from *T. pseudonana*
481 (Lhcf8) was used for modelling. In contrast, Nagao et al. (2019a) attributed the subunits of the
482 tetramer to Lhcf1, a constituent of the trimeric complexes in other centrics. However, since the
483 resolution of the PSII-FCP supercore structures is at 3.0 and 3.6 Å, respectively, slight
484 variations in the electron densities between monomers might suggest that the tetramers consist
485 of several, very similar Lhc proteins. Concerning the monomeric subunits, one (FCP-D) turned
486 out to be an antenna protein of the Lhcr group (Pi et al. 2019). The others could not be
487 unambiguously identified. Very recently, a low resolution structure of the PSII-FCP complex
488 of *T. pseudonana* was published (Arshad et al. 2021). The overall arrangement with three
489 monomeric and two oligomeric FCP complexes resembled closely the structure of PSII from
490 *Ch. gracilis*. However, the oligomeric FCPs appeared as trimers, not as tetramers, in accordance
491 with the trimeric FCPs from the free FCP pool of *T. pseudonana*.

492 In summary, surprisingly, three different oligomeric states of FCPs exist besides monomeric
493 Lhcs when considering pennate and centric diatoms together, whereas in plants only trimeric
494 complexes (LHCII) and dimers (LHCI) are found. The recently available structures of a
495 supercore from centrics (*Chaetoceros*) (Nagao et al. 2019a; Pi et al. 2019) and an FCP from
496 pennates (*Phaeodactylum*) (Wang et al. 2019) were combined by Wang et al. (2020) into a
497 model where the supercore having tetrameric FCPs bound is surrounded by a pool of dimeric
498 FCPs. However, for the centrics *C. meneghiniana* as well as *T. pseudonana* trimeric FCPs were
499 demonstrated by imaging methods to constitute the pool of peripheral FCPs and the PSII
500 associated FCPs, respectively (Röding et al. 2018, Arshad et al. 2021). In addition, no data are
501 available about the oligomeric state of the remaining FCPs in pennates (built of other subunits
502 than Lhcf4), and no structure of the PSII supercomplex is available. Using biochemical
503 analyses, trimers were found in both groups of diatoms. In addition, in centric diatoms
504 nonamers of specific polypeptide composition are present (Beer et al. 2006; Grouneva et al.
505 2011; Nagao et al. 2013a). For PSI the situation is much more clear, since only monomeric
506 Lhcs are attached (Veith and Büchel 2007; Nagao et al. 2019b; Nagao et al. 2020, Xu et al.
507 2020).



508

509

510 **Figure 2**

511 A: Scheme of the PSII-FCP supercore complex according to Nagao et al. (2019a) and Pi et al.
 512 (2019). The core of PSII, with the reaction center proteins D1 and D2 and the inner antenna
 513 proteins CP43 and CP47, is almost identical in plants and diatoms and shown in grey. PSII is a
 514 dimer, surrounded by FCP complexes on both sides. FCP-A, the subunit of both tetramers (ST
 515 and MT) was modelled using *T. pseudonana* Lhcf8 in case of Pi et al. (2019) and identified as
 516 Lhcf1 by Nagao et al. (2019a). Note that in *T. pseudonana* these complexes are trimeric (Arshad
 517 et al. 2021). FCP-D corresponds to Lhca2, a protein of the Lhcr group. FCP-E and FCP-F could
 518 not be identified.

519 B: Overlay of one of the monomers of the S-tetramer (taken from pdb 6JLU, 3.0 Å resolution,
 520 Pi et al. 2019) with one monomer of the dimeric FCP out of Lhcf4 of *P. tricornutum* (pdb
 521 6A2W, 1.8 Å resolution, Wang et al. 2019). Since the structure of the M-tetramers as well as
 522 the tetramers by Nagao et al. (2019a) (pdb 6J40, 3.6 Å) closely resembles the shown structure,
 523 they are omitted from the comparison. The protein backbone is depicted in grey (6JLU) and
 524 white (6A2W), respectively. The pigments in (nearly) identical sites in both complexes are
 525 omitted for the dimeric FCP and shown in colors for the ST-FCP: Chl *a* in green and Chl *c* in
 526 blue, whereby Chl 405, which was attributed to Chl *a* in the dimeric FCP and to Chl *c* in the
 527 tetramers, is shown in blue-green. The Chl *a* not found in the dimeric FCP (and M-tetramers),
 528 but in S-tetramers is depicted in light-green. The four Fx molecules present in identical
 529 locations in the dimer and the tetramers are shown in orange, whereas the Fx molecule present
 530 only in the tetrameric FCPs is shown in yellow. Fx306 is oriented more perpendicular to the
 531 membrane plane in the FCP dimer, whereas it adopts a different orientation in some subunits
 532 of the tetramers; both orientations are given in brown color. The additional Fx molecules and
 533 the Dd only present in the dimer are shown in red and black, respectively. The left panel shows
 534 the same complexes as the right panel, but turned by 180° around the y-axis.
 535

536

537 **2.5 Molecular structure of FCPs**

538 The first molecular structure at high resolution (1.8 Å) of a dimeric FCP of Lhcf4 from *P.*
 539 *tricornutum* became available recently (Wang et al. 2019), and the overall features were
 540 confirmed for the FCPs within the PSII-FCP and PSI-FCP supercomplexes (Nagao et al. 2019a;

541 Pi et al. 2019; Nagao et al. 2020) (Fig. 2B). The overall protein scaffold structure of FCP
542 monomers is similar to that of LHCII monomers (for an overview see Büchel 2019). The helices
543 where sequence conservation is high, i.e. helix 1 and 3, adopt an almost identical configuration
544 in FCP vs. LHCII, whereas helix 2 has a slightly different location and tilt that also differs
545 between the FCP-dimer from *P. tricornutum* and the FCP-tetramers from *Ch. gracilis* found in
546 PSII-supercomplexes. The complex from *P. tricornutum* was crystallized as a dimer, whereby
547 the connection between the monomers was due to strong interactions between helices 2. This
548 ‘head to head’ configuration has not been shown before for any member of the Lhc family,
549 since e.g. Lhca1/Lhc4 dimers of plant PSI interact in a ‘head to tail’ configuration (Ben-Shem
550 et al. 2003). Similarly, the monomers of the M- and S-tetramer in the PSII-FCP supercore
551 complexes are associated ‘head to tail’. In contrast to LHCII, where helices 3 come close to the
552 stromal surface, the subunits of the tetramers are turned by 180° in comparison to LHCII, so
553 that helices 1 approach closest to the stromal side (Nagao et al. 2019a; Pi et al. 2019). Although
554 helices 1 and 3 are almost identical in FCP and LHCII, the dimer and the tetramers are arranged
555 in a way that these helices adopt a slightly different tilt with respect to the membrane plane
556 compared to the arrangement in the trimeric LHCII (Liu et al. 2004; Standfuss et al. 2005;
557 Büchel 2019).

558 Seven Fx, one Dd, seven Chl *a*, and two Chl *c* per monomer were fitted into the electron density
559 map of the *P. tricornutum* FCP-dimer (Wang et al. 2019), whereas in the tetrameric FCPs of
560 *Ch. gracile* only six Fx, but nine (M-tetramer) or ten Chl molecules (S-tetramer) were found
561 (Pi et al. 2019; Wang et al. 2019) (Fig. 2B), and, as stated above, the variability is even larger
562 in PSI associated Lhc. In general, the Chl:carotenoid ratio is much lower than in plant LHCII.
563 As already anticipated from sequence comparisons and based on spectroscopy data
564 (Premvardhan et al. 2010), six of the Chl binding sites are highly conserved between LHCII
565 and FCP, with the central Fx molecules arranged close to helix 1 and 3 similarly to the luteins
566 in LHCII (Liu et al. 2004; Standfuss et al. 2005). One Dd was fitted in a more peripherally
567 located density in the *P. tricornutum* FCP-dimer, but was not found in any of the *Ch. gracilis*
568 tetramers (Fig. 2B). The porphyrin rings of Chl *c* and Chl *a* are rather similar in structure, so
569 Chl *c* can only be distinguished from Chl *a* due to the planarity of the C18=C17 double bonds
570 and the lack of phytol in Chl *c*, which requires a high resolution electron density map to resolve.
571 In the diatom FCP-tetramers close to PSII, three Chl *c* were assigned, the additional one being
572 Chl *c*405 (nomenclature according to Wang et al. 2019), a binding site that had been assigned
573 to Chl *a* in the FCP-dimer of *P. tricornutum* only for reasons of pigment stoichiometry (Wang
574 et al. 2019). Surprisingly, Chl *c*403 and Chl *c*408 reside in the strongly conserved binding sites

575 603 (Chl *c*403) and 612 (Chl *c*408), occupied by Chl *a* in case of LHCII. Both Chl *c*'s are in
576 close contact with Fx molecules, which are bound in places where no carotenoids are found in
577 case of LHCII. All carotenoid molecules in FCP are in *all-trans* configuration, and all have Chl
578 *a* molecules in close vicinity (3.1 to 3.6 Å). Whereas the Chl binding sites are highly conserved
579 between the FCP-dimer and the FCP-tetramer structures, only four Fx are found in identical
580 places to LHC carotenoids (Fig. 2B), including those in the lutein binding sites. The Fx
581 interacting with one of the Chl *c* in the Chl *a*/Chl *c*/Chl *a* clusters (Fx306) is oriented almost
582 perpendicular to the membrane plane in the FCP-dimers and in some subunits of the tetramers,
583 whereas it is oriented in an angle of almost 45° in others. Two Fx are found in totally different
584 locations in tetramers compared to the dimer. The most peculiar Fx is Fx304 in the FCP-dimer,
585 running almost parallel to the membrane plane on the stromal side. This Fx is missing in the
586 FCP-tetramers.

587 **2.6 Excitation energy transfer in FCPs**

588 Pigment ratios of around 6-8 Chl *a* : 2-3 Chl *c* : 6-8 Fx were reported for the different diatom
589 FCP complexes (which represented rather the main, free pool of FCP complexes), depending
590 on growth condition, isolation procedure and species (Papagiannakis et al. 2005; Beer et al.
591 2006; Lepetit et al. 2007; Joshi-Deo et al. 2010; Lepetit et al. 2010; Gundermann and Büchel
592 2012; Nagao et al. 2013b). More evident differences were reported concerning the PSI
593 associated Lhc antennae proteins: For both centric and pennate diatoms the Chl *c*/Fx ratio was
594 lower, whereas the (Dd+Dt)/Fx ratio was strongly increased (Lepetit et al. 2007; Veith and
595 Büchel 2007; Veith et al. 2009; Lepetit et al. 2010; Juhas and Büchel 2012). The Chl *c*/Fx ratio
596 was even lower when *P. tricornutum* was grown under red light (Bína et al. 2016). Whereas
597 this pigmentation is obviously due to the presence of the different Lhcf and Lhcr polypeptides,
598 respectively, nothing is known so far about the pigmentation of the gene products of *RedCaps*,
599 *Lhcy* or *Lhcz* that have been solely analyzed on genetic level so far. Even for Lhcx proteins the
600 question of whether they are pigmented remains open, since they have not been isolated as
601 single proteins so far. However, their high similarity to the pigmented LhcSR proteins of green
602 algae (Bonente et al. 2011) is a strong argument for diatom Lhcx proteins binding pigments
603 (see “*Photosynthetic light reactions in diatoms. II. The dynamic regulation of the various light*
604 *reactions*”).

605 In FCPa and FCPb complexes of *C. meneghiniana*, two differently bound Chl *c* molecules were
606 identified by Resonance Raman spectroscopy (Premvardhan et al. 2010) and also in 2D
607 spectroscopy by their different transfer times (Songaila et al. 2013; Gelzinis et al. 2015), in

608 agreement with the numbers although not the locations found in the crystal structure for *P.*
609 *tricornutum* Lhcf4 (Wang et al. 2019). In all FCPs isolated so far, the Q_Y absorption of FCPs is
610 at relatively short wavelength (~671 nm), excluding close excitonic interactions between Chl *a*
611 molecules as verified by CD spectra, where no excitonic interactions are visible in the Q_Y
612 (Büchel 2003; Szábo et al. 2008; Joshi-Deo et al. 2010). The fact that the strong Chl *a*
613 interaction of a610/a611/a612 visible in LHCII (Novoderezhkin et al. 2004) is broken by Chl *c*
614 in FCPs, also due to slightly different arrangement of Chl *a*401 (FCP) compared to Chl *a*611
615 (LHCII), is also in line with the lack of excitonic interactions. Thus, delocalized excited states
616 are missing, which contribute to the robustness of energy transfer in the flexible protein
617 environment e.g. in LHCII of vascular plants. FCP complexes, in contrast, seem to use subtle
618 changes in protein scaffold conformation to switch frequently into low-energy states with
619 improved light-harvesting properties as shown for FCPa from *C. meneghiniana* (Krüger et al.
620 2017).

621 Fx is actively involved in energy transfer to Chl *a*. Fx is special since it has a carbonyl moiety
622 in conjugation with the polyene backbone. Carotenoids are in principle able to transfer energy
623 from both their lowest singlet excited states, i.e. S₁ and S₂, but direct absorption into S₁ is
624 forbidden due to their symmetry. In Fx an additional excited state with an intramolecular charge
625 transfer (ICT) character exists. This ICT state can be coupled to the S₁ state, and plays a major
626 role in carotenoid-Chl energy transfer (Bautista et al. 1999; Vaswani et al. 2003; Zigmantas et
627 al. 2004; Papagiannakis et al. 2005; Premvardhan et al. 2005; Gelzinis et al. 2015; West et al.
628 2018). In addition, Fx displays an extreme bathochromic shift upon protein binding, extending
629 the absorption from 390 nm up to 580 nm. More ‘blue’, ‘green’ and ‘red’ absorbing Fx
630 molecules were detected in FCPa as well as in FCPb from *C. meneghiniana* (Premvardhan et
631 al. 2008; Premvardhan et al. 2009; Premvardhan et al. 2010) using Stark and Resonance Raman
632 spectroscopy, but could so far not be attributed to certain Fx molecules in the structure. ‘Blue’
633 and ‘red’ Fx were also demonstrated for whole cells of *C. meneghiniana* and *P. tricornutum*
634 using electrochromic shift measurements (Szábo et al. 2010). Excitation energy transfer from
635 Fx to Chl *a* proceeds mainly via the S₁/S_{ICT} state in FCPs, whereby the transfer to the Q_Y state
636 of Chl *a* has a time constant of 0.6 ps in FCPa of *C. meneghiniana* (Papagiannakis et al. 2005;
637 Gildenhoff et al. 2010a). The transfer for the Fx S₂ state directly into the Q_X state of Chl *a* is
638 even faster with <150 fs (Gildenhoff et al. 2010a). For *P. tricornutum*, two routes using the
639 S₁/S_{ICT} state were determined recently, whereby the slower (~ 6 ps) route uses the S₁ part of the
640 potential surface of the S₁/S_{ICT} equilibrium (West et al. 2018). The fast Fx to Chl *a* transfer is

641 possible due to the arrangement of Fx and Chl *a*: each Fx has an Chl *a* molecule in close vicinity
642 as stated above. Fx also acts as an efficient quencher of Chl *a* triplets (Di Valentin et al. 2012).
643 Fx-Fx transfer with a time constant of 25 ps was measured using FCPa of *C. meneghiniana*
644 (Gildenhoff et al. 2010a; Gildenhoff et al. 2010b). However, no pair of Fx molecules can be
645 pinpointed in the structures responsible for this route of excitation energy transfer.

646 No energy transfer from Fx to Chl *c* was observed within the limit of instrumentation of pump-
647 probe as well as 2D spectroscopy for *C. meneghiniana* FCPs (Papagiannakis et al. 2005;
648 Gildenhoff et al. 2010a; Songaila et al. 2013; Gelzinis et al. 2015). 2D spectroscopy also
649 revealed that the two Chl *c* have different time constants for energy transfer into Chl *a*, both
650 reactions being extremely fast with 60 fs and less, respectively (Songaila et al. 2013; Gelzinis
651 et al. 2015). This is in agreement with the close contact of Chl *c* and Chl *a*, allowing fast
652 excitation energy transfer between these pigments. Judging from the structure, also the Fx/Chl
653 *c* arrangement is, however, perfectly suited for fast excitation energy transfer. If present, it has
654 to be even faster than Chl *c*-Chl *a* transfer in order to have escaped detection.

655 The differences might be due to the fact that spectroscopically mainly the trimeric FCPs from
656 *C. meneghiniana* were analyzed, whereas structural data come from the dimeric FCP of *P.*
657 *tricornutum*. The contradictions between the structure and the wealth of spectroscopic data were
658 recently highlighted (Gelzinis et al. 2020). More structures are evidently needed in order to
659 fully understand excitation energy transfer in FCP.

660 In the PSII-FCP supercore complex, energy pathways have only been deduced from the
661 structure so far. The distances between Chls imply that the S-tetramers funnel energy into CP47,
662 one of the inner antenna proteins of PSII, via a Chl *a* binding subunit called PsbG that is not
663 present in vascular plant PSII, and into FCP-D (Fig. 2A). From the latter the energy can be
664 transferred to CP43, the inner antenna on the opposite side of the PSII reaction center compared
665 to CP47. The M-tetramer might transfer energy via FCP-E and FCP-D also into the Chls bound
666 to CP43. FCP-F is rather peripheral and thus probably delivers energy mainly to the M-tetramer.

667 Also for the PSI-FCP complexes an excitation energy transfer network was proposed, with
668 pathways in between the inner ring of Lhc proteins as well as pathways from the more
669 peripheral antenna into the inner ring and from there to the core. Since the methods to prepare
670 supercore complexes in sufficient amounts for ultrafast spectroscopy are available now, these
671 pathways will probably be elucidated in more detail in future.

672

673

674 **Outlook**

675 The recently obtained structures of PSII and PSI supercomplexes allow for the first time
676 detailed insights into particular steric features of the whole light harvesting system and the
677 excitation energy routes in diatoms. We need more of these structures, obtained from diatoms
678 in different acclimation states but also from different species. This way, we may reveal the
679 localization of the Lhcx proteins as well of those proteins which so far have only been found
680 on the genetic level, such as *Lhcz* or *Redcap*. More of these studies will also enable us to resolve
681 some so far existing discrepancies about the composition and oligomerisation states of FCPs
682 obtained either by classical biochemical preparations or by crystallization approaches. In
683 addition, the dynamic interaction between thylakoid lipid domains and thylakoidal protein
684 complexes in diatoms is a field which is as yet largely understudied and would also profit from
685 sophisticated imaging approaches. In this regard, we also need to better understand biogenesis
686 of thylakoid membranes and photosynthetic complexes. Recently, first insights regarding the
687 insertion of FCPs in *P. tricornutum* have been obtained. Alb3b, a protein functioning in the
688 insertion and assembly of thylakoid membrane protein complexes in plants, was demonstrated
689 to be essential for FCP assembly (Nymark et al. 2019). On the other hand, the chloroplast signal
690 recognition particle protein CpSRP54, involved in targeting LHC to the chloroplast membrane
691 in plants and green algae, is not involved in FCP accumulation but important for the insertion
692 of plastid encoded thylakoid membrane proteins (Nymark et al 2021). This paves the way for
693 future studies on FCP assembly, but to fully understand this process, also the enzymes working
694 in Fx and Chl *c* synthesis still need to be identified.

695

696

697 **References**

- 698
- 699 Abida H, Dolch L-J, Mei C, Villanova V, Conte M, Block MA, . . . Maréchal E (2015) Membrane
700 glycerolipid remodeling triggered by nitrogen and phosphorus starvation in *Phaeodactylum*
701 *tricornutum*. *Plant Physiol* 167 (1):118-136.
- 702 Alberte RS, Friedman AL, Gustafson DL, Rudnick MS, Lyman H (1981) Light harvesting systems of brown
703 algae and diatoms. Isolation and characterization of chlorophyll a/c and chlorophyll
704 a/fucoxanthin pigment protein complexes. *Biochimica et Biophysica Acta* 635:304-316.
- 705 Anderson JM (1999) Insights into the consequences of grana stacking of thylakoid membranes in
706 vascular plants: a personal perspective. *Funct Plant Biol* 26 (7):625-639.
- 707 Arshad R, Calvaruso C, Boekema EJ, Büchel C, Kouřil R (2021) Revealing the architecture of the
708 photosynthetic apparatus in the diatom *Thalassiosira pseudonana*. *Plant Physiol* 186 (4):2124-
709 2136.
- 710 Bailleul B, Rogato A, de Martino A, Coesel S, Cardol P, Bowler C, . . . Finazzi G (2010) An atypical member
711 of the light-harvesting complex stress-related protein family modulates diatom responses to
712 light. *Proc Natl Acad Sci USA* 107 (42):18214-18219.
- 713 Bautista JA, Connors RE, Raju BB, Hiller RG, Sharples FP, Gosztola D, . . . Frank HA (1999) Excited state
714 properties of peridinin: observation of a solvent dependence of the lowest excited singlet state
715 lifetime and spectral behavior unique among carotenoids. *J Phys Chem B* 103 (41):8751-8758.
- 716 Beer A, Gundermann K, Beckmann J, Büchel C (2006) Subunit composition and pigmentation of
717 fucoxanthin-chlorophyll proteins in diatoms: Evidence for a subunit involved in diadinoxanthin
718 and diatoxanthin binding. *Biochemistry* 45 (43):13046-13053.
- 719 Ben-Shem A, Frolow F, Nelson N (2003) Crystal structure of plant photosystem I. *Nature* 426
720 (6967):630-635.
- 721 Berkaloff C, Caron L, Rousseau B (1990) Subunit organization of PSI particles from brown algae and
722 diatoms: polypeptide and pigment analysis. *Photosynth Res* 23:181-193.
- 723 Biggins J, Bruce D (1989) Regulation of excitation energy transfer in organisms containing phycobilins.
724 *Photosynth Res* 20 (1):1-34.
- 725 Bína D, Herbstová M, Gardian Z, Vácha F, Litvín R (2016) Novel structural aspect of the diatom thylakoid
726 membrane: lateral segregation of photosystem I under red-enhanced illumination. *Sci Rep*
727 6:25583.
- 728 Bojko M, Olchawa-Pajor M, Chyc M, Goss R, Schaller-Laudel S, Latowski D Acclimatization of
729 *Thalassiosira pseudonana* photosynthetic membranes to environmental temperature
730 changes. In: *Proceedings of the 3rdWorld Congress on New Technologies, 2017*. doi:DOI:
731 10.11159/icepr17.120
- 732 Bojko M, Olchawa-Pajor M, Goss R, Schaller-Laudel S, Strzałka K, Latowski D (2019) Diadinoxanthin de-
733 epoxidation as important factor in the short-term stabilization of diatom photosynthetic
734 membranes exposed to different temperatures. *Plant Cell Environ* 42:1270-1286.
- 735 Bonente G, Ballottari M, Truong TB, Morosinotto T, Ahn TK, Fleming GR, . . . Bassi R (2011) Analysis of
736 Lhcsr3, a protein essential for feedback de-excitation in the green alga *Chlamydomonas*
737 *reinhardtii*. *PLoS Biol* 9 (1):e1000577.
- 738 Brakemann T, Schlormann W, Marquardt J, Nolte M, Rhiel E (2006) Association of fucoxanthin
739 chlorophyll a/c-binding polypeptides with photosystems and phosphorylation in the centric
740 diatom *Cyclotella cryptica*. *Protist* 157 (4):463-475.
- 741 Browse J, Warwick N, Somerville CR, Slack CR (1986) Fluxes through the prokaryotic and eukaryotic
742 pathways of lipid synthesis in the '16:3' plant *Arabidopsis thaliana*. *Biochem J* 235 (1):25-31.
- 743 Büchel C (2003) Fucoxanthin-chlorophyll proteins in diatoms: 18 and 19 kDa subunits assemble into
744 different oligomeric states. *Biochemistry* 42:13027-13034.
- 745 Büchel C (2015) Evolution and function of light harvesting proteins. *J Plant Physiol* 172:62-75.
- 746 Büchel C (2020) Light harvesting complexes in chlorophyll c-containing algae. *BBA-Bioenergetics*
747 1861:148027.

748 Buck JM, Sherman J, Bártulos CR, Serif M, Halder M, Henkel J, . . . Lepetit B (2019) Lhc proteins provide
749 photoprotection via thermal dissipation of absorbed light in the diatom *Phaeodactylum*
750 *tricornutum*. Nat Commun 10 (1):4167.

751 Calvaruso C, Rokka A, Aro E-M, Büchel C (2020) Specific Lhc proteins are bound to PSI or PSII
752 supercomplexes in the diatom *Thalassiosira pseudonana*. Plant Physiol
753 DOI:10.1104/pp.20.00042.

754 Canavate JP, Armada I, Rios JL, Hachero-Cruzado I (2016) Exploring occurrence and molecular diversity
755 of betaine lipids across taxonomy of marine microalgae. Phytochemistry 124:68-78.

756 Caron L, Brown J (1987) Chlorophyll-carotenoid protein complexes from the diatom *Phaeodactylum*
757 *tricornutum*: spectrophotometric, pigment and polypeptide analyses. Plant Cell Physiol 28:775-
758 785.

759 Cho SH, Thompson G (1987) On the metabolic relationships between monogalactosyldiacylglycerol and
760 digalactosyldiacylglycerol molecular species in *Dunaliella salina*. J Biol Chem 262 (16):7586-
761 7593.

762 Croce R, van Amerongen H (2020) Light harvesting in oxygenic photosynthesis: Structural biology
763 meets spectroscopy. Science 369 (6506):eaay2058.

764 Di Valentin M, Buchel C, Giacometti GM, Carbonera D (2012) Chlorophyll triplet quenching by
765 fucoxanthin in the fucoxanthin-chlorophyll protein from the diatom *Cyclotella meneghiniana*.
766 Biochem Biophys Res Commun 427 (3):637-641.

767 Dodson VJ, Dahmen JL, Mouget J-L, Leblond JD (2013) Mono- and digalactosyldiacylglycerol
768 composition of the marennine-producing diatom, *Haslea ostrearia*: Comparison to a selection
769 of pennate and centric diatoms. Phycol Res 61 (3):199-207.

770 Dodson VJ, Mouget J-L, Dahmen JL, Leblond JD (2014) The long and short of it: temperature-dependent
771 modifications of fatty acid chain length and unsaturation in the galactolipid profiles of the
772 diatoms *Haslea ostrearia* and *Phaeodactylum tricornutum*. Hydrobiologia 727 (1):95-107.

773 Dorrell RG, Gile G, Mccallum G, Méheust R, Baptiste EP, Klinger CM, . . . Bowler C (2017) Chimeric
774 origins of ochrophytes and haptophytes revealed through an ancient plastid proteome. Elife
775 6:e23717.

776 Engelken J, Funk C, Adamska I (2012) The extended light-harvesting complex (LHC) protein superfamily:
777 Classification and evolutionary dynamics. in R Burnap, W Vermaas, eds, Functional Genomics
778 and Evolution of Photosynthetic Systems, Volume 33, Springer:265-284.

779 Eppard M, Rhiel E (1998) The genes encoding light-harvesting subunits of *Cyclotella cryptica*
780 (Bacillariophyceae) constitute a complex and heterogeneous family. Mol Genet Genomics 260
781 (4):335-345.

782 Falkowski PG, Fenchel T, DeLong EF (2008) The microbial engines that drive earth's biogeochemical
783 cycles. Science 320 (5879):1034-1039.

784 Fawley MW (1989) A new form of chlorophyll c involved in light-harvesting. Plant Physiol 91 (2):727-
785 732.

786 Fawley MW, Grossman AR (1986) Polypeptides of a light-harvesting complex of the diatom
787 *Phaeodactylum tricornutum* are synthesized in the cytoplasm of the cell as precursors. Plant
788 Physiol 81:149-155.

789 Flori S, Jouneau P-H, Bailleul B, Gallet B, Estrozi LF, Moriscot C, . . . Finazzi G (2017) Plastid thylakoid
790 architecture optimizes photosynthesis in diatoms. Nat Commun 8:15885.

791 Friedman AL, Alberte RS (1984) A diatom light-harvesting pigment-protein complex. Plant Physiol
792 76:483-489.

793 Gardian Z, Litvín R, Bína D, Vácha F (2014) Supramolecular organization of fucoxanthin–chlorophyll
794 proteins in centric and pennate diatoms. Photosynth Res 121 (1):79-86.

795 Gelzinis A, Augulis R, Büchel C, Robert B, Valkunas L (2021) Confronting FCP structure with ultrafast
796 spectroscopy data: evidence for structural variations. Phys Chem Chem Phys 23 (2):806-821.

797 Gelzinis A, Butkus V, Songaila E, Augulis R, Gall A, Büchel C, . . . Valkunas L (2015) Mapping energy
798 transfer channels in fucoxanthin–chlorophyll protein complex. BBA-Bioenergetics 1847
799 (2):241-247.

800 Ghazaryan A, Akhtar P, Garab G, Lambrev PH, Büchel C (2016) Involvement of the LhcX protein Fcp6 of
801 the diatom *Cyclotella meneghiniana* in the macro-organisation and structural flexibility of
802 thylakoid membranes. *BBA-Bioenergetics* 1857 (9):1373-1379.

803 Gildenhoff N, Amarie S, Gundermann K, Beer A, Büchel C, Wachtveitl J (2010a) Oligomerization and
804 pigmentation dependent excitation energy transfer in fucoxanthin-chlorophyll proteins. *BBA-*
805 *Bioenergetics* 1797 (5):543-549.

806 Gildenhoff N, Herz J, Gundermann K, Büchel C, Wachtveitl J (2010b) The excitation energy transfer in
807 the trimeric fucoxanthin–chlorophyll protein from *Cyclotella meneghiniana* analyzed by
808 polarized transient absorption spectroscopy. *Chem Phys* 373 (1-2):104-109.

809 Goss R, Greifenhagen A, Bergner J, Volke D, Hoffmann R, Wilhelm C, Schaller-Laudel S (2017) Direct
810 isolation of a functional violaxanthin cycle domain from thylakoid membranes of higher plants.
811 *Planta* 245 (4):793-806.

812 Goss R, Latowski D, Grzyb J, Vieler A, Lohr M, Wilhelm C, Strzalka K (2007) Lipid dependence of
813 diadinoxanthin solubilization and de-epoxidation in artificial membrane systems resembling
814 the lipid composition of the natural thylakoid membrane. *BBA-Biomembranes* 1768 (1):67-75.

815 Goss R, Lohr M, Latowski D, Grzyb J, Vieler A, Wilhelm C, Strzalka K (2005) Role of hexagonal structure-
816 forming lipids in diadinoxanthin and violaxanthin solubilization and de-epoxidation.
817 *Biochemistry* 44 (10):4028-4036.

818 Goss R, Nerlich J, Lepetit B, Schaller S, Vieler A, Wilhelm C (2009) The lipid dependence of
819 diadinoxanthin de-epoxidation presents new evidence for a macrodomain organization of the
820 diatom thylakoid membrane. *J Plant Physiol* 166:1839-1854.

821 Grouneva I, Rokka A, Aro EM (2011) The thylakoid membrane proteome of two marine diatoms
822 outlines both diatom-specific and species-specific features of the photosynthetic machinery. *J*
823 *Proteome Res* 10 (12):5338-5353.

824 Guglielmi G, Lavaud J, Rousseau B, Etienne AL, Houmard J, Ruban AV (2005) The light-harvesting
825 antenna of the diatom *Phaeodactylum tricornutum* - Evidence for a diadinoxanthin-binding
826 subcomplex. *FEBS J* 272 (17):4339-4348.

827 Gugliemelli L (1984) Isolation and characterization of pigment-protein particles from the light-
828 harvesting complex of *Phaeodactylum tricornutum*. *Biochimica et Biophysica Acta* 766:45-50.

829 Gundermann K, Büchel C (2012) Factors determining the fluorescence yield of fucoxanthin-chlorophyll
830 complexes (FCP) involved in non-photochemical quenching in diatoms. *BBA-Bioenergetics*
831 1817 (7):1044-1052.

832 Gundermann K, Schmidt M, Weisheit W, Mittag M, Büchel C (2013) Identification of several sub-
833 populations in the pool of light harvesting proteins in the pennate diatom *Phaeodactylum*
834 *tricornutum*. *BBA-Bioenergetics* 1827 (3):303-310.

835 Gundermann K, Wagner V, Mittag M, Büchel C (2019) Fucoxanthin-chlorophyll protein complexes of
836 the centric diatom *Cyclotella meneghiniana* differ in LhcX1 and LhcX6_1 content. *Plant Physiol*
837 179:779–1795.

838 Guschina IA, Harwood JL (2006) Lipids and lipid metabolism in eukaryotic algae. *Prog Lip Res* 45 (2):160-
839 186.

840 Herbstová M, Bína D, Kaňa R, Vácha F, Litvín R (2017) Red-light phenotype in a marine diatom involves
841 a specialized oligomeric red-shifted antenna and altered cell morphology. *Sci Rep* 7 (1):1-10.

842 Herbstová M, Bína D, Koník P, Gardian Z, Vácha F, Litvín R (2015) Molecular basis of chromatic
843 adaptation in pennate diatom *Phaeodactylum tricornutum*. *BBA-Bioenergetics* 1847 (6–7):534-
844 543.

845 Ikeda Y, Komura M, Watanabe M, Minami C, Koike H, Itoh S, . . . Satoh K (2008) Photosystem I
846 complexes associated with fucoxanthin-chlorophyll-binding proteins from a marine centric
847 diatom, *Chaetoceros gracilis*. *BBA-Bioenergetics* 1777 (4):351-361.

848 Ikeda Y, Yamagishi A, Komura M, Suzuki T, Dohmae N, Shibata Y, . . . Satoh K (2013) Two types of
849 fucoxanthin-chlorophyll-binding proteins I tightly bound to the photosystem I core complex in
850 marine centric diatoms. *BBA-Bioenergetics* 1827:529-539.

851 Joshi-Deo J, Schmidt M, Gruber A, Weisheit W, Mittag M, Kroth PG, Büchel C (2010) Characterization
852 of a trimeric light-harvesting complex in the diatom *Phaeodactylum tricornutum* built of FcpA
853 and FcpE proteins. J Exp Bot 61:3079-3087.

854 Juhas M, Büchel C (2012) Properties of photosystem I antenna protein complexes of the diatom
855 *Cyclotella meneghiniana*. J Exp Bot 63:3673-3681.

856 Kalaji HM, Schansker G, Ladle RJ, Goltsev V, Bosa K, Allakhverdiev SI, . . . Zivcak M (2014) Frequently
857 asked questions about in vivo chlorophyll fluorescence: practical issues. Photosynth Res 122
858 (2):121-158.

859 Kansy M, Volke D, Sturm L, Wilhelm C, Hoffmann R, Goss R (2020) Pre-purification of diatom pigment
860 protein complexes provides insight into the heterogeneity of FCP complexes. BMC Plant Biol
861 20 (1):456. doi:10.1186/s12870-020-02668-x.

862 Kern J, Guskov A (2011) Lipids in photosystem II: Multifunctional cofactors. J Photochem Photobiol B
863 104 (1):19-34.

864 Kirchhoff H (2014) Diffusion of molecules and macromolecules in thylakoid membranes. BBA-
865 Bioenergetics 1837 (4):495-502.

866 Kirchhoff H, Hall C, Wood M, Herbstová M, Tsabari O, Nevo R, . . . Reich Z (2011) Dynamic control of
867 protein diffusion within the granal thylakoid lumen. Proc Natl Acad Sci USA 108 (50):20248.

868 Kirchhoff H, Schöttler MA, Maurer J, Weis E (2004) Plastocyanin redox kinetics in spinach chloroplasts:
869 evidence for disequilibrium in the high potential chain. BBA-Bioenergetics 1659 (1):63-72.

870 Kraay GW, Zapata M, Veldhuis MJW (1992) Separation of chlorophylls c1, c2, and c3 of marine
871 phytoplankton by reversed-phase-C18-high-performance liquid chromatography. J Phycol
872 28:708-712.

873 Krüger TP, Malý P, Alexandre MT, Mančal T, Büchel C, Van Grondelle R (2017) How reduced excitonic
874 coupling enhances light harvesting in the main photosynthetic antennae of diatoms. Proc Natl
875 Acad Sci USA 114 (52):E11063-E11071.

876 Kühlbrandt W, Wang DN, Fujiyoshi Y (1994) Atomic model of plant light-harvesting complex by electron
877 crystallography. Nature 367 (6464):614-621.

878 Latowski D, Akerlund HE, Strzalka K (2004) Violaxanthin de-epoxidase, the xanthophyll cycle enzyme,
879 requires lipid inverted hexagonal structures for its activity. Biochemistry 43 (15):4417-4420.

880 Latowski D, Kruk J, Burda K, Skrzynecka-Jaskier M, Kostecka-Gugala A, Strzalka K (2002) Kinetics of
881 violaxanthin de-epoxidation by violaxanthin de-epoxidase, a xanthophyll cycle enzyme, is
882 regulated by membrane fluidity in model lipid bilayers. Eur J Biochem 269 (18):4656-4665.

883 Lavaud J, Rousseau B, Etienne AL (2003) Enrichment of the light-harvesting complex in diadinoxanthin
884 and implications for the nonphotochemical fluorescence quenching in diatoms. Biochemistry
885 42 (19):5802-5808.

886 Lepetit B, Goss R, Jakob T, Wilhelm C (2012) Molecular dynamics of the diatom thylakoid membrane
887 under different light conditions. Photosynth Res 111 (1-2):245-257.

888 Lepetit B, Volke D, Gilbert M, Wilhelm C, Goss R (2010) Evidence for the existence of one antenna-
889 associated, lipid-dissolved, and two protein-bound pools of diadinoxanthin cycle pigments in
890 diatoms. Plant Physiol 154:1905-1920.

891 Lepetit B, Volke D, Szabo M, Hoffmann R, Garab GZ, Wilhelm C, Goss R (2007) Spectroscopic and
892 molecular characterization of the oligomeric antenna of the diatom *Phaeodactylum*
893 *tricornutum*. Biochemistry 46 (34):9813-9822.

894 Levitan O, Chen M, Kuang X, Cheong KY, Jiang J, Banal M, . . . Dai W (2019) Structural and functional
895 analyses of photosystem II in the marine diatom *Phaeodactylum tricornutum*. Proc Natl Acad
896 Sci USA 116 (35):17316.

897 Lohr M, Wilhelm C (1999) Algae displaying the diadinoxanthin cycle also possess the violaxanthin cycle.
898 Proc Natl Acad Sci USA 96 (15):8784-8789

899 Liu ZF, Yan HC, Wang KB, Kuang TY, Zhang JP, Gui LL, . . . Chang WR (2004) Crystal structure of spinach
900 major light-harvesting complex at 2.72 angstrom resolution. Nature 428 (6980):287-292.

901 Mann DG, Vanormelingen P (2013) An inordinate fondness? The number, distributions, and origins of
902 diatom species. J Eukaryot Microbiol 60 (4):414-420.

903 Mock T, Kroon BMA (2002) Photosynthetic energy conversion under extreme conditions - I: important
904 role of lipids as structural modulators and energy sink under N-limited growth in Antarctic sea
905 ice diatoms. *Phytochemistry* 61 (1):41-51.

906 Murata N, Siegenthaler P-A (1998) Lipids in photosynthesis: an overview. In: Siegenthaler PA MN (ed)
907 Lipids in photosynthesis: structure, function and genetics. Kluwer Academic Publishers,
908 Dordrecht, pp 1-20

909 Nagao R, Kato K, Ifuku K, Suzuki T, Kumazawa M, Uchiyama I, . . . Akita F (2020) Structural basis for
910 assembly and function of a diatom photosystem I-light-harvesting supercomplex. *Nat Commun*
911 11 (1):2481.

912 Nagao R, Kato K, Suzuki T, Ifuku K, Uchiyama I, Kashino Y, . . . Akita F (2019a) Structural basis for energy
913 harvesting and dissipation in a diatom PSII–FCPII supercomplex. *Nat Plants* 5 (8):890-901.

914 Nagao R, Takahashi S, Suzuki T, Dohmae N, Nakazato K, Tomo T (2013a) Comparison of oligomeric
915 states and polypeptide compositions of fucoxanthin chlorophyll a/c-binding protein complexes
916 among various diatom species. *Photosynth Res* 117 (1-3):281-288.

917 Nagao R, Tomo T, Noguchi E, Suzuki T, Okumura A, Narikawa R, . . . Ikeuchi M (2012) Proteases are
918 associated with a minor fucoxanthin chlorophyll a/c-binding protein from the diatom,
919 *Chaetoceros gracilis*. *BBA-Bioenergetics* 1817 (12):2110-2117.

920 Nagao R, Ueno Y, Akita F, Suzuki T, Dohmae N, Akimoto S, Shen J-R (2019b) Biochemical
921 characterization of photosystem I complexes having different subunit compositions of
922 fucoxanthin chlorophyll a/c-binding proteins in the diatom *Chaetoceros gracilis*. *Photosynth*
923 *Res* 140 (2):141-149.

924 Nagao R, Yokono M, Akimoto S, Tomo T (2013b) High excitation energy quenching in fucoxanthin
925 chlorophyll a/c-binding protein complexes from the diatom *Chaetoceros gracilis*. *J Phys Chem*
926 *B* 117:6888–6895.

927 Nagao R, Yokono M, Ueno Y, Shen J-R, Akimoto S (2018) Low-energy chlorophylls in fucoxanthin
928 chlorophyll a/c-binding protein conduct excitation energy transfer to photosystem I in
929 diatoms. *J Phys Chem B* 123 (1):66-70.

930 Neilson JA, Durnford DG (2010) Structural and functional diversification of the light-harvesting
931 complexes in photosynthetic eukaryotes. *Photosynth Res* 106 (1-2):57-71.

932 Novoderezhkin VI, Palacios MA, Van Amerongen H, Van Grondelle R (2004) Energy-transfer dynamics
933 in the LHCII complex of higher plants: modified redfield approach. *J Phys Chem B* 108
934 (29):10363-10375.

935 Nymark M, Grønbech Hafskjold MC, Volpe C, Fonseca DdM, Sharma A, Tsirvouli E, . . . Bones AM (2021)
936 Functional studies of CpSRP54 in diatoms show that the mechanism of thylakoid protein
937 insertion differs from that in plants and green algae. *Plant J* 106 (1):113-132.

938 Nymark M, Valle KC, Brembu T, Hancke K, Winge P, Andresen K, . . . Bones AM (2009) An integrated
939 analysis of molecular acclimation to high light in the marine diatom *Phaeodactylum*
940 *tricornutum*. *PLoS One* 4 (11):e7743.

941 Nymark M, Volpe C, Hafskjold MCG, Kirst H, Serif M, Vadstein O, . . . Winge P (2019) Loss of ALBINO3b
942 insertase results in truncated light-harvesting antenna in diatoms. *Plant Physiol* 181 (3):1257-
943 1276.

944 Oka K, Ueno Y, Yokono M, Shen J-R, Nagao R, Akimoto S (2020) Adaptation of light-harvesting and
945 energy-transfer processes of a diatom *Phaeodactylum tricornutum* to different light qualities.
946 *Photosynth Res* <https://doi.org/10.1007/s11120-020-00714-1>.

947 Owens T (1988) Light-harvesting antenna systems in the chlorophyll a/c-containing algae. In: Stevens
948 SE BD (ed) Light-energy transduction in photosynthesis: higher plants and bacterial models. .
949 Rockville, Maryland, pp 122-136

950 Owens TG, World ER (1986) Light-harvesting function in the diatom *Phaeodactylum tricornutum*: I.
951 Isolation and characterization of pigment-protein-complexes. *Plant Physiol* 80:732-738.

952 Papagiannakis E, van Stokkum IHM, Fey H, Büchel C, van Grondelle R (2005) Spectroscopic
953 characterization of the excitation energy transfer in the fucoxanthin-chlorophyll protein of
954 diatoms. *Photosynth Res* 86 (1-2):241-250.

955 Pi X, Zhao S, Wang W, Liu D, Xu C, Han G, . . . Shen J-R (2019) The pigment-protein network of a diatom
956 photosystem II-light-harvesting antenna supercomplex. *Science* 365:eaax4406.

957 Premvardhan L, Bordes L, Beer A, Büchel C, Robert B (2009) Carotenoid structures and environments
958 in trimeric and oligomeric fucoxanthin chlorophyll a/c proteins from Resonance Raman
959 Spectroscopy. *J Phys Chem B* 113 (37):12565-12574.

960 Premvardhan L, Papagiannakis E, Hiller RG, Van Grondelle R (2005) The charge-transfer character of
961 the S₀→ S₂ transition in the carotenoid peridinin is revealed by Stark spectroscopy. *J Phys
962 Chem B* 109 (32):15589-15597.

963 Premvardhan L, Robert B, Beer A, Buchel C (2010) Pigment organization in fucoxanthin chlorophyll
964 a/c(2) proteins (FCP) based on resonance Raman spectroscopy and sequence analysis. *BBA-
965 Bioenergetics* 1797 (8):1647-1656.

966 Premvardhan L, Sandberg DJ, Fey H, Birge RR, Büchel C, van Grondelle R (2008) The charge-transfer
967 properties of the S state of fucoxanthin in solution and in fucoxanthin chlorophyll-a/c protein
968 (FCP) based on stark spectroscopy and molecular-orbital theory. *J Phys Chem B* 112
969 (37):11838-11853.

970 Pyszniak AM, Gibbs SP (1992) Immunocytochemical localization of photosystem I and the fucoxanthin-
971 chlorophyll-a/c light-harvesting complex in the diatom *Phaeodactylum tricornutum*.
972 *Protoplasma* 166 (3-4):208-217.

973 Röding A, Boekema E, Büchel C (2018) The structure of FCPb, a light-harvesting complex in the diatom
974 *Cyclotella meneghiniana*. *Photosynth Res* 135 (1-3):203-211.

975 Rousch JM, Bingham SE, Sommerfeld MR (2003) Changes in fatty acid profiles of thermo-intolerant and
976 thermo-tolerant marine diatoms during temperature stress. *J Exp Mar Biol Ecol* 295 (2):145-
977 156.

978 Schaller-Laudel S, Latowski D, Jemiola-Rzeminska M, Strzalka K, Daum S, Bacia K, . . . Goss R (2017)
979 Influence of thylakoid membrane lipids on the structure of aggregated light-harvesting
980 complexes of the diatom *Thalassiosira pseudonana* and the green alga *Mantoniella squamata*.
981 *Physiol Plant* 160 (3):339-358.

982 Schaller S, Latowski D, Jemiola-Rzeminska M, Wilhelm C, Strzalka K, Goss R (2010) The main thylakoid
983 membrane lipid monogalactosyldiacylglycerol (MGDG) promotes the de-epoxidation of
984 violaxanthin associated with the light-harvesting complex of photosystem II (LHCII). *BBA-
985 Bioenergetics* 1797 (3):414-424.

986 Schober AF, Rio Bartulos C, Bischoff A, Lepetit B, Gruber A, Kroth PG (2019) Organelle studies and
987 proteome analyses of mitochondria and plastids fractions from the diatom *Thalassiosira
988 pseudonana*. *Plant Cell Physiol* 60 (8):1811-1828.

989 Singer SJ, Nicolson GL (1972) The Fluid Mosaic Model of the Structure of Cell Membranes. *Science* 175
990 (4023):720.

991 Smith BM, Melis A (1988) Photochemical apparatus organization in the diatom *Cylindrotheca
992 fusiformis*: Photosystem stoichiometry and excitation distribution in cells grown under high
993 and low irradiance. *Plant Cell Physiol* 29:761-769.

994 Songaila E, Augulis Rn, Gelzinis A, Butkus V, Gall A, Büchel C, . . . Valkunas L (2013) Ultrafast energy
995 transfer from chlorophyll c 2 to chlorophyll a in fucoxanthin–chlorophyll protein complex. *J
996 Phys Chem Lett* 4 (21):3590-3595.

997 Standfuss J, van Scheltinga ACT, Lamborghini M, Kühlbrandt W (2005) Mechanisms of photoprotection
998 and nonphotochemical quenching in pea light-harvesting complex at 2.5Å resolution. *EMBO J*
999 24 (5):919-928.

1000 Strzepek RF, Harrison PJ (2004) Photosynthetic architecture differs in coastal and oceanic diatoms.
1001 *Nature* 431 (7009):689-692.

1002 Szábo M, Lepetit B, Goss R, Wilhelm C, Mustardy L, Garab G (2008) Structurally flexible macro-
1003 organization of the pigment-protein complexes of the diatom *Phaeodactylum tricornutum*.
1004 *Photosynth Res* 95 (2-3):237-245.

1005 Szábo M, Premvardhan L, Lepetit B, Goss R, Wilhelm C, Garab G (2010) Functional heterogeneity of the
1006 fucoxanthins and fucoxanthin-chlorophyll proteins in diatom cells revealed by their

1007 electrochromic response and fluorescence and linear dichroism spectra. *Chem Phys* 373:110-
1008 114.

1009 Taddei L, Chukhutsina V, Lepetit B, Stella GR, Bassi R, van Amerongen H, . . . Falciatore A (2018) Dynamic
1010 changes between two LHCX-related energy quenching sites control diatom photoacclimation.
1011 *Plant Physiol* 177:953-965.

1012 Thamatrakoln K, Bailleul B, Brown CM, Gorbunov MY, Kustka AB, Frada M, . . . Bidle KD (2013) Death-
1013 specific protein in a marine diatom regulates photosynthetic responses to iron and light
1014 availability. *Proc Natl Acad Sci USA* 110 (50):20123-20128.

1015 Vaswani HM, Hsu C-P, Head-Gordon M, Fleming GR (2003) Quantum chemical evidence for an
1016 intramolecular charge-transfer state in the carotenoid peridinin of peridinin- chlorophyll-
1017 protein. *J Phys Chem B* 107 (31):7940-7946.

1018 Veith T, Brauns J, Weisheit W, Mittag M, Büchel C (2009) Identification of a specific fucoxanthin-
1019 chlorophyll protein in the light harvesting complex of photosystem I in the diatom *Cyclotella*
1020 *meneghiniana*. *BBA-Bioenergetics* 1787 (7):905-912.

1021 Veith T, Büchel C (2007) The monomeric photosystem I-complex of the diatom *Phaeodactylum*
1022 *tricornutum* binds specific fucoxanthin chlorophyll proteins (FCPs) as light-harvesting
1023 complexes. *BBA-Bioenergetics* 1767 (12):1428-1435.

1024 Vieler A, Wilhelm C, Goss R, Sub R, Schiller J (2007) The lipid composition of the unicellular green alga
1025 *Chlamydomonas reinhardtii* and the diatom *Cyclotella meneghiniana* investigated by MALDI-
1026 TOF MS and TLC. *Chem Phys Lipids* 150 (2):143-155.

1027 Wang W, Yu L-J, Xu C, Tomizaki T, Zhao S, Umena Y, . . . Suga MJS (2019) Structural basis for blue-green
1028 light harvesting and energy dissipation in diatoms. *Science* 363 (6427):eaav0365.

1029 Wang W, Zhao S, Pi X, Kuang T, Sui S-F, Shen J-R (2020) Structural features of the diatom photosystem
1030 II-light-harvesting antenna complex. *FEBS J* 287:2191–2200.

1031 West RG, Bina D, Fuciman M, Kuznetsova V, Litvín R, Polívka T (2018) Ultrafast multi-pulse transient
1032 absorption spectroscopy of fucoxanthin chlorophyll a protein from *Phaeodactylum*
1033 *tricornutum*. *BBA-Bioenergetics* 1859 (5):357-365.

1034 Wilhelm C, Goss R, Garab G (2020) The fluid-mosaic membrane theory in the context of photosynthetic
1035 membranes: Is the thylakoid membrane more like a mixed crystal or like a fluid? *J Plant Physiol*
1036 252:153246.

1037 Xu C, Pi X, Huang Y, Han G, Chen X, Qin X, . . . Shen JR (2020) Structural basis for energy transfer in a
1038 huge diatom PSI-FCPI supercomplex. *Nat Commun* 11 (1):5081.

1039 Yan X, Chen D, Xu J, Zhou C (2011) Profiles of photosynthetic glycerolipids in three strains of
1040 *Skeletonema* determined by UPLC-Q-TOF-MS. *J Appl Phycol* 23 (2):271-282.

1041 Yongmanitchai W, Ward OP (1993) Positional distribution of fatty acids, and molecular species of polar
1042 lipids, in the diatom *Phaeodactylum tricornutum*. *J Gen Microbiol* 139 (3):465-472.

1043 Zhu SH, Green BR (2010) Photoprotection in the diatom *Thalassiosira pseudonana*: Role of LI818-like
1044 proteins in response to high light stress. *BBA-Bioenergetics* 1797 (8):1449-1457.

1045 Zigmantas D, Hiller RG, Sharples FP, Frank HA, Sundström V, Polívka T (2004) Effect of a conjugated
1046 carbonyl group on the photophysical properties of carotenoids. *Phys Chem Chem Phys* 6
1047 (11):3009-3016.

1048

1049

1050 **Acknowledgements**

1051 BB acknowledges financial support from the European Research Council (ERC) under the
1052 European Union Horizon 2020 research and innovation program (grant agreement no. 715579).
1053 BL thanks the Deutsche Forschungsgemeinschaft (LE3358/3-2) and the Baden-Württemberg
1054 Stiftung (Elite program) for financial support. CB acknowledges support by the European
1055 Union's Horizon 2020 research and innovation programme under the Marie Skłodowska-Curie
1056 grant agreement No 675006 and from the Deutsche Forschungsgemeinschaft, grant Bu 812 10-
1057 1. DAC thanks the Canada Research Chairs and Natural Science and Engineering Research
1058 Council of Canada for support. JL thanks the Centre National de la Recherche Scientifique-
1059 CNRS, the Natural Sciences and Engineering Research Council of Canada-NSERC (Discovery
1060 and Northern Supplement grants), the Canada First Research Excellence Fund-Sentinelle Nord,
1061 and the strategic research cluster Québec-Océan for their financial support. All authors thank
1062 the reviewer for valuable suggestions.